厚生労働科学研究費補助金　医療機器開発（ナノテクノロジー等）総合推進研究事業
（分担）研究報告書

肝臓に対する新規 DDS を活用した経口遺伝子治療法の開発

和田　猛[1)]
[1)] 東京大学大学院新領域創成科学研究科　メディカルゲノム専攻

研究要旨

A 型二重らせん構造を有する二本鎖核酸に選択的に結合し、その熱力学的安定性を向上させ、ヌクレアーゼによる分解を阻害するカチオン性人工ペプチドの合成を検討した。種々のカチオン性官能基を有するオリゴペプチドを二本鎖核酸に結合させ、二重鎖の熱的安定性に及ぼす効果を評価した。また、カチオン性ペプチドが siRNA に結合することにより、ヌクレアーゼ耐性が顕著に向上することを見出した。さらに、カチオン性ペプチドは RNAi 活性に大きな影響を及ぼさないことが示された。

A.研究目的

核酸医薬の経口治療薬の開発を目指し、二本鎖核酸に強く結合し、生体内でその高次構造を安定化し、様々な分解酵素による分解を阻害する人工分子の合成をおこなう。さらに、その分子にビタミン E を結合させ、核酸医薬と複合体を形成させることにより、ビタミン E の代謝経路を利用した肝細胞特異的なデリバリーを可能にする新規 DDS の開発をおこなう。

B.研究方法

A型二重らせん構造を有する二本鎖核酸のメジャーグルーブの幅に合致し、核酸のリン酸ジエステル部位の負電荷と効果的に相互作用可能な正電荷を有するカチオン性人工ペプチド(図 1)をデザインし、合成する。

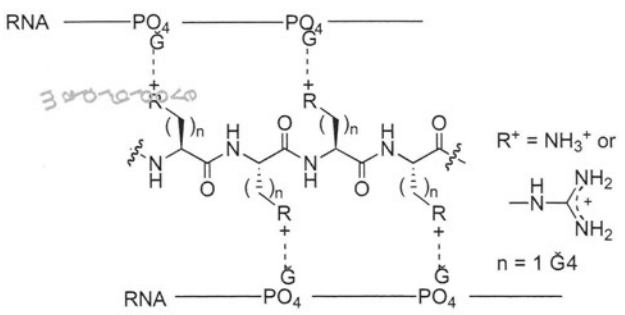

図 1.　RNA 二重鎖に結合するカチオン性ペプチドの構造

合成したカチオン性ペプチドと核酸二重鎖の相互作用を T_m（二重鎖の熱的安定性）、CD スペクトル（二重鎖の構造変化）、蛍光異方性（結合力の定量）などの物理化学的測定により評価する。さらに、二本鎖 RNA とカチオン性ペプチド複合体のヌクレアーゼ耐性の評価をおこなう。また、カチオン性ペプチドが RNAi 活性に及ぼす影響について調べる。

（倫理面への配慮）
該当なし

C.研究結果

A型二重らせん構造を有する二本鎖核酸のメジャーグルーブに結合可能なカチオン性分子として、図 1 に示す、アミノ基またはグアニジノ基を有し、側鎖メチレン長が 1ー4 のオリゴペプチド（カチオン性残基数＝8）の合成を達成した。RNA 二重鎖とカチオン性オリゴペプチドの相互作用を解析するために、自己相補的な塩基配列を有する RNA 二重鎖、$r(CGCGAAUUCGCG)_2$ とカチオン性ペプチドの複合体を形成させ、T_m 値を測定したところ、アミノ基を有するオリゴペプチドの中では L-2,4-ジアミノブタン酸オリゴマー(Dab_8)が ΔT_m=14.0 °C、グアニジノ基を有するも

のでは2-アミノ-4-グアニジノブタン酸オリゴマー(Agb$_8$)がΔT_m=16.2 °Cと二重鎖の安定化効果が最も高かった(図2)。先行研究で我々が開発したオリゴジアミノグルコースは、同様の条件下で4.1 °CのT_m値の上昇にとどまったことから、カチオン性ペプチドのRNA二重鎖に対する安定化の効果が大きいことが確認された。また、CDスペクトルの測定から、これらのカチオン性ペプチドはA型RNA二重鎖の高次構造に変化を与えないこともわかった。

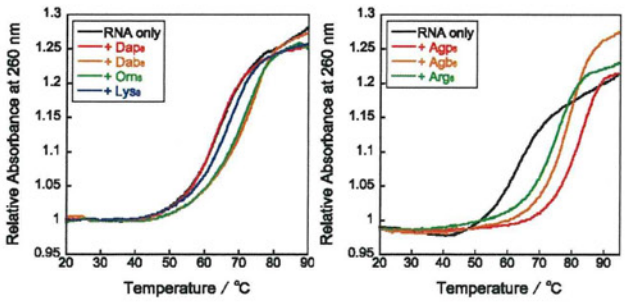

図2.　Tm値の測定（左：アミノ基、右：グアニジノ基）

次に、同様の塩基配列を有するRNAオリゴマーの5'-末端に蛍光基としてフルオレセインを導入し、蛍光異方性測定により、カチオン性ペプチドとRNA二重鎖の解離定数（*K*d値）を測定した(図3)。Dab$_8$、Agp$_8$それぞれの*K*d値は0.071μM、0.046μMであり、既知のRNA結合性タンパク質と同等の値を示し、RNA二重鎖に対して強く結合することが示された。

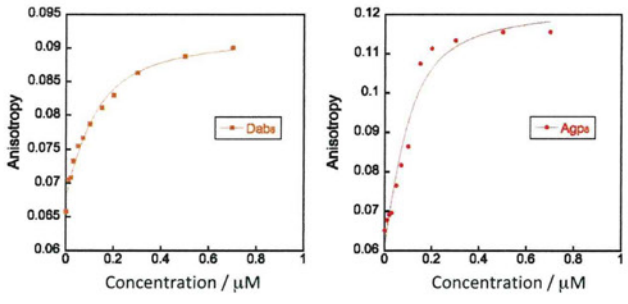

図3.　蛍光異方性測定（左：Dab$_8$、右：Agp$_8$）

次に、マウス・ヒト・ラットのアポリポ蛋白B(ApoB)を標的とするsiRNA(21量体)に対し、1、3、5当量のカチオン性ペプチドを添加して複合体を形成させ、二本鎖RNAを切断するエンドヌクレアーゼであるRNase Aで処理した後に、ポリアクリルアミドゲル電気泳動によって残存するsiRNAをエチジウムブロミド染色によって検出した。siRNA単独では完全に分解される条件でもDab$_8$、Agp$_8$が存在する場合には当量依存的にsiRNAの分解が抑制されることが確認できた。

最後に、カチオン性ペプチドがRNAi活性に及ぼす影響について調べた。ApoBを標的とするsiRNAを用い、1、3、5当量のカチオン性ペプチドを添加して複合体を形成させ、ラット肝がん細胞McA-RH7777にリポフェクタミンを用いてsiRNA-ペプチド複合体を導入し、RNAi活性を測定した。Dab$_8$は1当量から3当量まで添加してもカチオン性ペプチド非存在下の活性と同等であったのに対し、Agp$_8$では当量依存的にRNAi活性の低下が観測された(図4)。Agp$_8$はsiRNAにより強く結合するため、RNAiの活性が阻害されたと考えられる。

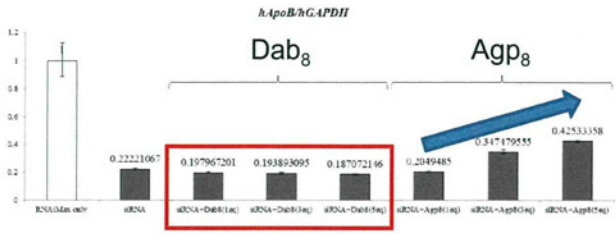

図4.　ペプチド複合体（1, 3, 5当量）のRNAi活性

D.考察

本研究でデザイン、合成したカチオン性ペプチド、Dab$_8$とAgp$_8$は、二本鎖RNAの熱安定性を顕著に向上させることがわかった。これらのペプチドのカチオン性残基間の距離(Dab$_8$: 9Å、Agp$_8$: 11Å)は、A型構造を有する二本鎖RNAのメジャーグルーブ幅に近く、グルーブの両側のリン酸と効果的に相互作用することが可能である。また、これらのペプチドが二本鎖RNAに結合することにより、RNase A耐性が獲得されるが、特にDab$_8$の場合、RNAi活性は阻害しないことが示された。Dab$_8$は二本鎖RNA結合性タンパク質と同等の結合親和性を有するため、RNaseの結合を阻害する

が、RISC 形成は阻害しないと考えられる。一方、siRNA に対してより強い結合親和性を有する Agp8 は、過剰量用いた場合に RISC 形成を阻害するために、RNAi 活性が低下したと考えられる。

E.結論

本研究では、A 型核酸二重鎖との高い結合親和性を有するチオン性ペプチドの合成に成功した。これらのペプチドが有する高い二本鎖 RNA の熱安定化効果、RNase A 耐性および RNAi 活性を阻害しないという性質は、siRNA 医薬の経口剤への応用を可能にする、優れた特性であるといえる。今後はカチオン性ペプチドとビタミン E が結合した siRNA と複合体を形成させ、腸管内での安定性や肝臓へのデリバリー効率を検証する予定である。

F.健康危険情報

本研究で合成したカチオン性ペプチドは生体適合性の高い分子であると考えられるが、新規化合物であり、今後細胞毒性や安全性に関する試験を適宜おこなう必要がある。

G.研究発表

1. 論文発表

1. Nukaga Y, Yamada K, Ogata T, Oka N, Wada T. Stereocontrolled solid-phase synthesis of phosphorothioate oligoribonucleo- tides using 2′-O-(2-cyanoethoxymethyl)-nucleoside 3′-O-oxazaphospholidine monomers. J Org Chem 2012; 77: 7913–7922.
2. Iwamoto N, Oka N, Wada T. Stereocontrolled synthesis of oligodeoxyribo- nucleoside boranophosphates by an oxazaphos-pholidine approach using acid-labile N-protecting groups. Tetrahedron Lett 2012; 53: 4361–4364.
3. Oka N, Takayama Y, Ando K, Wada T. Synthesis of nucleoside 5′-borano-phosphorothioate derivatives using an H-boranophosphonate monoester as a precursor. Bioorg Med Chem Lett 2012; 22: 4571–4574.
4. Oka N, Sato K, Wada T. Recent progress in the synthesis of glycosyl phosphate derivatives. Trends in Glycosci Glycotechnol 2012; 24: 152-168.
5. Maeda Y, Iwata R, Wada T. Synthesis of novel oligocationic peptides which bind to A-type nucleic acid duplexes. Peptide cience 2011 2012; 231-232 .
6. Maeda Y, Iwata R, Wada T. Synthesis and properties of cationic oligopeptides with different side chain lengths that bind to RNA duplexes. Bioorg Med Chem 2013; 21: 1717–1723.

2.学会発表

1. 和田猛. 医薬品を志向した機能性キラル核酸の創成. 第 40 回バイオインターフェース, 東京, 2012.11.12
2. 和田猛. Stereocontrolled synthesis and properties of P-chiral oligonucleotides. 8th Annual Meeting of the Oligonucleotide Therapeutics Society 2012, Boston, 2012.10.29
3. 前田雄介, 岩田倫太朗, 和田猛. Synthesis of novel oligocationic peptides which bind to RNA duplexes. 第 39 回国際核酸化学シンポジウム, 名古屋, 2012.11.15
4. 植原渉, 日浦信吾, 東田廉平, 岡夏央, 和田猛. Solid-phase synthesis of boron-containing DNA analogues by the H-boranophosphonate method. 第 39 回国際核酸化学シンポジウム, 名古屋, 2012.11.15
5. 和田猛, 影山雅幸, 新井浩一郎, 内山直樹. Synthesis and properties of 2′-O-haloethox-

ymethyl RNA. 第 39 回国際核酸化学シンポジウム, 名古屋, 2012.11.15

6. 土井明子, 岩田倫太朗, 和田猛. 核酸二重鎖結合性オリゴジアミノマンノースの合成とその性質. 日本化学会第 93 春季年会, 草津, 2013.3.23
7. 前田雄介, 岩田倫太朗, 和田猛. RNA 二重鎖を認識する新規カチオン性人工ペプチドの合成. 日本化学会第 93 春季年会, 草津 , 2013.3.23
8. 額賀陽平, 竹下文隆, 落谷孝広, 和田猛. 2'-O-CEM 基を有するオキサザホスホリジンモノマーを用いた PO/PS キメラオリゴリボヌクレオチドの立体選択的合成. 日本化学会第 93 春季年会, 草津, 2013.3.24
9. 前田雄介, 岩田倫太朗, 和田猛. Synthesis of novel oligocationic peptides binding to RNA duplexes. 第 49 回ペプチド討論会, 鹿児島, 2012.11.7

H.知的所有権の取得状況（予定を含む）

1.特許出願

発明の名称：二重鎖核酸結合剤、当該結合剤－二重鎖核酸複合体、当該複合体を含有する医薬品組成物、及び、当該複合体の製造方法.
出　願　人：東京医科歯科大学
発　明　人：横田隆徳, 仁科一隆, 和田猛, 前田雄介.
出 願 番 号：2013-057521
出　願　日：2013.3.21

2.実用新案登録

特になし

3.その他

特になし

厚生労働科学研究費補助金　医療機器開発（ナノテクノロジー等）総合推進研究事業
（分担）研究報告書

肝臓に対する新規 DDS を活用した経口遺伝子治療法の開発

小比賀　聡[1)]
[1)] 大阪大学大学院薬学研究科　生物有機化学

研究要旨

酸医薬の開発を試みた。アンチセンス核酸(ASO)に脂質を結合することによる有効な核酸デリバリー技術の開発を検討した。通常一本鎖であるASOに相補鎖核酸(cRNA)をハイブリダイズさせた新規の二本鎖ASO(dsASO)を開発した。この方法により、相補鎖側に脂質等デリバリーに用いるための生体内誘導分子をASO主鎖の有効性に影響を与えることなく結合することが可能となり、二本鎖ASOの有効性は静脈投与において１本鎖ASOの20-100倍という顕著な標的遺伝子有効性を示した。

A.研究目的

過酷な腸管内の RNA 分解酵素のある状況のなかで、核酸医薬の経腸管投与開発として siRNA の遺伝子抑制効果には限界があることが懸念され、今回より遺伝子抑制効果の高い新規の核酸医薬の開発を試みた。近年、siRNA より有効性の高い場合が明らかになった Gapmer 型の ASO を用いた遺伝子発現抑制方法は、その遺伝子治療のツールとして臨床応用が期待されている。DNA からなる ASO を導入すると、部分的に DNA-RNA のヘテロオリゴヌクレオチドを形成し、RNaseH によってこの部分が認識されて DNA-RNA のうちの RNA が分解され、蛋白質合成を抑制することができる。最近の RNaseH dependent pathway を用いた ASO の一種に、両末端に Locked Nucleic Acid (LNA)を導入し、中央部を DNA とした全長 12-13mer の短い ASO (LNA-DNA gapmer)の有効性が極めて高いことが知られている。しかし ASO 自体の多くは速やかに腎排泄されるため、必要投与量が増大して副作用の要因にもなり、標的臓器への有効なデリバリーが困難な状況である。

過去に行われてきた siRNA の研究において、ビタミン E を初めとした脂質を核酸に結合させることで肝への顕著な集積性が獲得され、肝特異的なデリバリーが可能となることが報告されている。それにより必要投与量が減少し、より効果的かつ安全な siRNA の全身投与を可能となる。この方法を ASO に応用すべく、我々は ASO の 3’末端に脂質を結合したが、その脂質がアンチセンス効果を直接阻害して有効性が得られなかった。そこで通常一本鎖核酸である ASO に相補鎖 RNA (cRNA)を結合させた dsASO を着想した。この方法は、相補鎖に脂質結合等の様々な誘導分子を結合させることで臓器特異的な送達を可能にする利点がある。

我々は、dsASO の有効性を確認して最適化すること、dsASO の特にデリバリーに関するメカニズムを解明することを目的として、横田グループ（東京医科歯科大）と共同で研究を行った。

B.研究方法

[dsASO の作成]

マウスアポリポ蛋白 B (apoB)を標的とした LNA-DNA gapmer 型の 13 塩基からなる一本鎖 ASO (ssASO)と、それと相補の配列を持つ 5’末端にビタミン E を結合させた cRNA (VE-cRNA)を合成した。下に配列及びその核酸化学修飾を示す。

ASO: 5’-GsCsaststsgsgstsastsTsCsA-3’

（大文字 : LNA、小文字 : DNA、s : 核酸間 S 化）

Toc-cRNA: 5’-Toc-usgsasAUACCAAUsgsc-3’

（大文字 ; RNA、小文字 : 2’-OMe RNA、s : 核酸間 S 化）

上記を 95°C で 5 分、その後 37°C で 1 時間静

置し、両者をハイブリダイズさせてビタミンE結合 dsASO (VE-dsASO)を作成した。また ssASO の 5'末端にビタミン E を直接結合させた VE-ssASO も合成した。

[マウスにおける VE-dsASO の標的遺伝子発現抑制効果の評価]

実験には、6~8 週令の ICR マウスを使用した。尾静脈から核酸を静注投与し、3 日後に採血した。その後冷却した生理食塩水にて脱血還流を施し、臓器を摘出した。組織及び血液サンプルを用いて、定量的 RT-PCR、血液検査等の各評価に供した。

[生体内での VE-dsASO の分布]

蛍光標識した ssASO と VE-dsASO を同様に投与し、生体イメージングシステム IVIS imaging system (Xenogen Corp., Hopkinton, MA)を用いて生体内での VE-dsASO の分布を観察した。

(倫理面への配慮)

動物実験は、動物愛護及び実験動物の適正管理、動物実験の適正化の観点から、大阪大学及び東京医科歯科大学の各動物実験委員会規定と動物実験指針に基づいて行った。

C.研究結果

1. VE-dsASO の標的遺伝子発現抑制効果

まず、VE-ssASO をマウスに静注した際の肝における標的遺伝子発現抑制効果を確認した(図 1)。

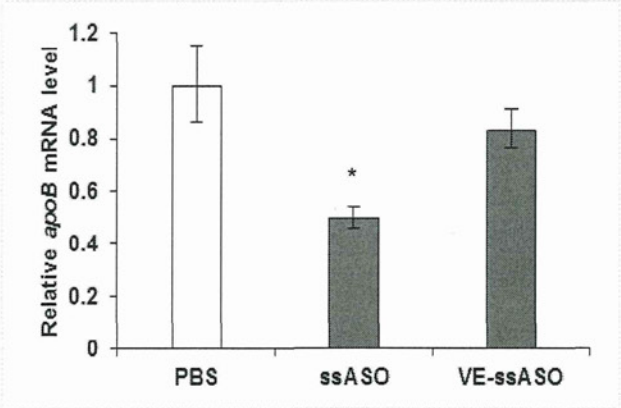

図1. マウスに対して ssASO と VE-ssASO を 0.75 mg/kg で静脈注射後、3 日後における肝での標的遺伝子の発現抑制効果($n = 3$, *: $P < 0.05$)

その結果、ビタミン E を直接アンチセンス核酸に結合することで、アンチセンス核酸の標的遺伝子発現抑制効果が著明に減弱することが示された。

次に、VE-dsASO を 0.02~0.75 mg/kg の投与量で同様にマウスに静注した際の標的遺伝子発現抑制効果を確認した(図 2)。その結果、Toc-dsASO が投与した用量依存性に標的遺伝子発現抑制効果を示すこと、標的遺伝子の発現を 50%抑制するのに必要な用量(ED_{50})が 0.036 mg/kg であることが分かった。ssASO の ED50 は 0.75 mg/kg であることから、VE-dsASO では ssASO のおよそ 5%であり、ssASO に直接ビタミン E を結合させた場合と異なり、二本鎖として間接的にビタミン E を結合させることにより大幅な有効性の上昇が認められた。

今回用いた ASO は apoB に対するものであり、そのまま高脂血症の治療薬となり得る。そこで、高脂肪食を 2 週間摂取させて作成した高脂血症モデルマウスに対して、高脂肪食を継続したまま週 1 回 ssASO または VE-dsASO をそれぞれ 0.09 若しくは 0.75 mg/kg 静注した。計 4 回投与し、最終投与の 3 日後の血清を用いて LDL コレステロール(LDLC)値を測定した (図 3)。その結果、特に VE-dsASO 投与群で LDLC 値の低下を認め、実際に VE-dsASO によって高脂血症に対する治療が可能になるものと考えられた。

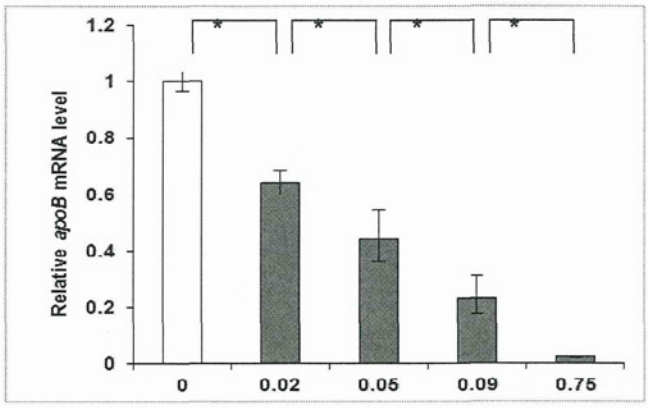

図 2. マウスに対して VE-dsASO を 0.02~0.75 mg/kg で静脈注射後、3 日後における肝での標的遺伝子の発現抑制効果($n = 3$, *: $P < 0.05$)

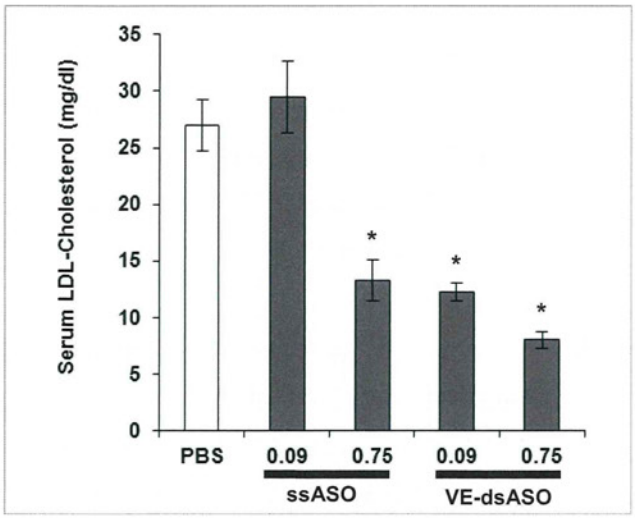

図 3. 高脂血症モデルマウスに対して ssASO と VE-dsASO を 0.09 若しくは 0.75 mg/kg で毎週静脈注射後、最終投与 3 日後における血中 LDL コレステロール値($n = 4$, *: $P < 0.05$)

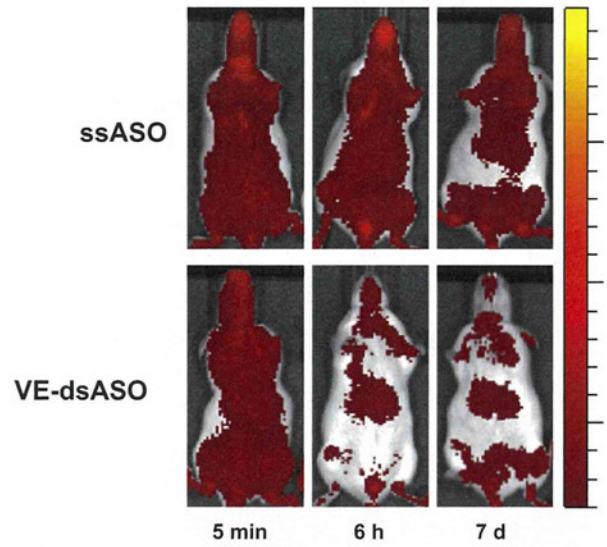

図 4. マウスに対して蛍光標識 ssASO と VE-dsASO を 0.75 mg/kg で静脈注射後、5 分、6 時間、7 日後における ASO の体内分布（IVIS imaging system を用いて撮影）

2. 生体内での VE-dsASO の分布

蛍光標識した VE-dsASO を 0.75 mg/kg で静注し、投与 5 分、6 時間、7 日後の体内における分布を IVIS imaging system を用いてそれぞれ撮像した（図 4）。その結果、ssASO において 7 日後でも生体内に広汎に分布しているのに対し、VE-dsASO では投与 6 時間後にはほぼ肝に集積しており、ビタミン E を結合することにより大幅な生体内分布の改善を確認できた。

3. 安全性の評価

VE-dsASO を 0.75 mg/kg で静注したマウスの血液サンプルの生化学的検査にて、VE-dsASO を静注投与した際の明らかな副作用は検出されなかった（表 1）。

	PBS only	VE-dsASO
BUN (mg/dl)	28.9 ± 1.6	26.5 ± 1.2
Cre (mg/dl)	0.16 ± 0.02	0.14 ± 0.01
AST (U/l)	73 ± 14	63 ± 3
ALT (U/l)	29 ± 2	35 ± 4

表 1. Toc-dsASO 静注時の血清生化学

D.考察

ASO のデリバリーは、主に核酸間のホスホロチオエート結合が担っていると考えられており、ナノパーティクルや脂質結合といったデリバリー因子を要する siRNA 等と異なりデリバリー用の素子が必要とされていない。しかし、臓器への集積性の点で ASO にも何らかのデリバリー因子を用いることが、ASO による効果向上・副作用軽減の両面で必要と思われる。

ビタミン E 結合機能核酸は、siRNA で報告があるように集積の点で肝へのデリバリーに際して有用であることが示されていた。そこでビタミン E を直接 ASO に結合してみたものの、逆に有効性を損ねる結果となった。そのため間接的にビタミン E を ASO に結合させるために、ASO に対する相補鎖を設計し、それにビタミン E を結合させることで、肝特異的なデリバリー及び効果の著明な向上という二点を成し遂げることができた。

今後の問題点として、腸管内の核酸分解酵素への対策が挙げられる。現状の VE-dsASO は特に cRNA 中央部の RNA に化学修飾を施しておらず、酵素耐性が不十分である。一方酵素耐性が強い化

学修飾を用いると ASO の効果に影響を及ぼすことが考えられ、ASO に影響を及ぼさずに酵素耐性を増すことができる有用な化学修飾の選択が必要になる。

E.結論

本開発中の経腸経リンパ管デリバリーシステムにおいて必要となる、より有効性の高いビタミン E 修飾核酸である VE-dsASO を設計・合成することができた。また、VE-dsASO 投与時の生体内分布において、ビタミン E を結合することにより肝特異的にデリバリーされることが確認された。また、本製剤の投与による安全性の検討から、マウスにおいて問題となる副作用は検出されなかった。今後 VE-dsASO を経腸投与する際に必要な化学修飾等の最適化を行う予定である。

F.健康危険情報

特記事項なし

G.研究発表

1. 論文発表

1. Hari Y, Osawa T, Obika S. Synthesis and Duplex-forming Ability of Oligonucleotides Containing 4'-Carboxythymidine Analogs. Org Biomol Chem 2012; 10: 9639-9649.
2. Kang JH, Tachibana Y, Obika S, Harada-Shiba M, Yamaoka T. Efficient Reduction of Serum Cholesterol by Combining a Liver-targeted Gene Delivery System with Chemically Modified Apolipoprotein B siRNA. J Control Release 2012; 163: 119–124.
3. Yahara A, Shrestha AR, Yamamoto T, Hari Y, Osawa T, Yamaguchi M, Nishida M, Kodama T, Obika S. Amido-Bridged Nucleic Acids (AmNAs): Synthesis, Duplex Stability, Nuclease Resistance, and In Vitro Antisense Potency. ChemBioChem 2012; 13: 2513-2516.
4. Yamamoto T, Yasuhara H, Wada F, Harada-Shiba M, Imanishi T, Obika S. Superior Silencing by 2',4'-BNA^{NC}-based Short Antisense Oligonucleotides Compared to 2',4'-BNA/LNA-based Apolipoprotein B Antisense Inhibitors. J Nucleic Acids Res 2012; 707323.
5. Wada S, Obika S, Shibata M, Yamamoto T, Nakatani M, Yamaoka T, Torigoe H, Shiba M. Development of a 2',4'-BNA/LNA Based siRNA for Dyslipidemia and Assessment of the Effects of its Chemical Modifications in vivo. Mol Ther-Nucleic Acids 2012; 1: e45.
6. Rahman SMA, Baba T, Kodama T, Islam MA, Obika S. Hybridizing Ability and Nuclease Resistance Profile of Backbone Modified Cationic Phosphorothioate Oligonucleotides. Bioorg Med Chem 2012; 20: 4098-4102.
7. Yamamoto T, Harada-Shiba M, Nakatani M, Wada S, Yasuhara H, Narukawa K, Sasaki K, Shibata M, Torigoe H, Yamaoka T, Imanishi T, Obika S. Cholesterol-lowering Action of BNA-based Antisense Oligonucleotides Targeting PCSK9 in Atherogenic Diet-induced Hypercholesterolemic Mice. Mol Ther-Nucleic Acids 2012; 1: e22.

2.学会発表

1. 原孝志, 兒玉哲也, 竹垣裕美, 森廣邦彦, 伊藤浩介, 小比賀聡. 2',4'-BNA/LNA-プリン塩基類縁体の二重鎖形成能に及ぼす二面角 χ の影響. 日本薬学会第 133 年会. 横浜. 2013.3.28
2. 森廣邦彦, 兒玉哲也, 肯特夫, 百合義大, Rakesh N. Veedu, 小比賀 聡. セレノメチレン架橋型人工核酸の開発と酸化還元スイッチへの応用. 日本薬学会第133年会. 横浜. 2013.3.28

3. 山本剛史, 斯波真理子, 安原秀典, 中谷萌夏, 小比賀聡. 高力価抗PCSK9アンチセンスの探索研究. 日本薬学会第133年会. 横浜. 2013.3.28
4. Mori K, Kodama T, Obika S. Synthesis and properties of a nucleic acid bearing boat-shaped pyranose sugar. 13th Tetrahedron Symposium - Asia Edition. 台北.2012.11.29, 30
5. Fujisaka A, Hari Y, Takuma H, Pang J, Imanishi T, Obika S. Synthesis and Property of Oligonucleotides Modified with 2',4'-BNANC Bearing Adenine, Guanine, Thymine and 5-Methylcytosine. 13th Tetrahedron Symposium - Asia Edition. 台北. 2012.11.27, 28
6. Yasuhara H, Yamamoto T, Obika S, Harada-Shiba M. Quantitative measurement of hepatic accumulation of phosphorothioated antisense oligonucleotides modified with bridged nucleic acids by elisa-based oligonucleotide detection method. 日本薬物動態学会　第27回年会. 東京. 2012.11.22
7. Kotobuki Y, Hari Y, Shrestha AR, Obika S. Synthesis and properties of guanidine-bridged nucleic acid: The effect of cationic bridge on duplex stability. The 39th Internatinal Symposium on Nucleic Acids Chemistry. 名古屋. 2012.11.16
8. Morihiro K, Kodama T, Obika S. Light-triggered Strand-displacement Reaction Using Recognition-base-changeable Nucleic Acids . The 39th Internatinal Symposium on Nucleic Acids Chemistry. 名古屋. 2012.11.15
9. 藤坂朱紀, 張功幸, 田熊寛子, 逢娟娟, 今西武, 小比賀聡. 核酸塩基部にアデニン、グアニン、チミン、5-メチルシトシンを持つ N-メチル-2',4'-BNA^{NC} の合成. 第 38 回反応と合成の進歩シンポジウム. 東京. 2012.11.6
10. Yahara A, Shrestha AR, Yamamoto T, Hari Y, Osawa T, Yamaguchi M, Nishida M, Kodama T, Obika S. Amido-bridged Nucleic Acid: Synthesis, Duplex Stability,Nuclease Resistance, and In Vitro Antisense Potency. 8th Annual Meeting of the Oligonucleotide Therapeutics Society. Boston. 2012.10.30
11. Yamamoto T, Yasuhara H, Nakatani M, Shibata MA, Obika S, Harada-Shiba M. Correction of Murine Hypertriglyceridemia by BNA Antisense Oligonucleotides Targeting Apolipoprotein C-III. 8th Annual Meeting of the Oligonucleotide Therapeutics Society. Boston. 2012.10.29
12. Yasuhara H, Yamamoto T, Nakatani M, Wada S, Torigoe H, Yamaoka T, Shibata MA, Imanishi T, Harada-Shiba M, Obika S. Design, Screening of Efficient BNA Antisense Okigonucleotides for PCSK9. 8th Annual Meeting of the Oligonucleotide Therapeutics Society. Boston. 2012.10.31
13. Wada S, Obika S, Shibata MA, Yamamoto T, Yamaoka T, Harada-Shiba M. In Vivo Assessment of the Chemical Modification of siRNA. 8th Annual Meeting of the Oligonucleotide Therapeutics Society.Boston. 2012.10.31
14. 安原秀典, 山本剛史, 和田俊輔, 中谷萌夏, 和田郁人, 鳥越秀峰, 山岡哲二, 柴田雅朗, 今西武, 斯波真理子, 小比賀聡. PCSK9阻害による家族性高コレステロール血症治療のための高機能性核酸医薬品の開発. アンチセンス・遺伝子・デリバリーシンポジウム2012. 仙台. 2012.9.24

15. 安原秀典, 山本剛史, 中谷萌夏, 柴田雅朗, 小比賀聡, 斯波真理子. 抗ApoC-IIIアンチセンス核酸による高トリグリセリド血症治療薬の開発. アンチセンス・遺伝子・デリバリーシンポジウム2012. 仙台. 2012.9.25
16. 壽悠太郎, 張功幸, Shrestha Ajaya Ram, 小比賀聡. 新規架橋型人工核酸の合成と機能評価;グアニジノ基による架橋部へのカチオン導入の効果. アンチセンス・遺伝子・デリバリーシンポジウム2012. 仙台. 2012.9.24
17. Hara T, Kodama T, Takegaki Y, Morihiro K, Ito KR, Obika S. Synthesis And Hybridization Property of Oligonucleotides Containing 2',4'-BNA-7-Deazaguanine Analog. XX IRT - 20th International Roundtable on Nucleosides. Montreal. 2012.8.6, 7
18. Mori K, Kodama T, Obika S. Investigation of the Factor Affecting the Duplex-Forming Ability of Boat-Shaped Glucopyranosyl Nucleic Acid. XX IRT - 20th International Roundtable on Nucleosides. Montreal. 2012.8.6, 7
19. 安原秀典, 山本剛史, 和田俊輔, 小比賀聡, 斯波真理子. PCSK9を標的とした人工核酸BNA搭載型アンチセンス医薬の開発. 第12回遺伝子・デリバリー研究会 夏季セミナー. 北九州. 2012.7.31
20. Yamamoto T, Yasuhara H, Nakatani M, Shibata MA, Obika S, Harada-Shiba M. Hypertriglyceridemic Mice Were Responsive to Apolipoprotein C-III-lowering Therapy by BNA-modified Antisense Oligonucleotides. 第44回日本動脈硬化学会総会・学術集会. 福岡. 2012.7.19
21. Yamamoto T, Harada-Shiba M, Nakatani M, Wada S, Yasuhara H, Narukawa K, Sasaki K, Shibata MA, Torigoe H, Yamaoka T, Imanishi T, Obika S. Screening and Selection of Efficient BNA-Modified anti-PCSK9 Antisenses. 第44回日本動脈硬化学会総会・学術集会. 福岡. 2012.7.20
22. 森廣邦彦, 兒玉哲也, 小比賀聡. 光刺激により認識塩基がグアニンからアデニンに変化するシン配向型人工核酸の開発. 日本ケミカルバイオロジー学会第7回年会. 京都. 2012.6.9
23. Osawa T, Hari Y, Obika S. Development of a Novel Bridged Nucleic Acid Based on Intramolecular Hydrogen Bond Formation. The 7th Seoul-Kyoto-Osaka Joint Symposium on Pharmaceutical Sciences for Young Scientists. 京都. 2012. 5.25
24. Mori K, Kodama T, Obika S. A Boat-Shaped Glucopyranosyl Nucleic Acid: Design, Synthesis and Hybridization Properties. The 7th Seoul-Kyoto-Osaka Joint Symposium on Pharmaceutical Sciences for Young Scientists. 京都. 2012. 5.24

H.知的所有権の取得状況（予定を含む）

1.特許取得（出願）

発明の名称：キメラ二重鎖核酸
出　願　人：東京医科歯科大学, 大阪大学
発　明　人：横田隆徳, 仁科一隆, 水澤英洋, 小比賀聡.
国際出願番号：PCT/JP2012/083180
出　願　日：2012.12.17

2.実用新案登録

特になし

3.その他

特になし

Ⅲ.　研究成果の刊行に関する一覧表

研究成果の刊行に関する一覧表

英文原著・症例報告

著　者　名	論　文　題　名	雑　誌　名	巻	頁	出版西暦年	GRANTへの謝辞の有無
Hirai T, Enomoto M, Machida A, Yamamoto M, Kuwahara H, Tajiri M, Hirai Y, Sotome S, Mizusawa H, Shinomiya K, Okawa A, Yokota T.	Intrathecal shRNA-AAV9 inhibits target protein expression in the spinal cord and dorsal root ganglia of adult mice.	Hum Gene Ther Methods.	23	119–127	2012	無
Nishina K, Mizusawa H, Yokota T.	Short interfering RNA and the central nervous system: development of nonviral delivery systems.	Expert Opin Drug Deliv.	10	289–292	2013	無
Takemoto H, Miyata K, Hattori S, Ishii T, Suma T, Uchida S, Nishiyama N, Kataoka K.	Acidic pH-Responsive siRNA conjugate for reversible carrier stability and accelerated endosomal escape with reduced IFNa-associated immune response.	Angew Chem Int Ed.	in press		2013	無
Maeda Y, Iwata R, Wada T.	Synthesis and properties of cationic oligopeptides with different side chain lengths that bind to RNA duplexes.	Bioorg Med Chem.	21	1717–1723	2013	有
Nukaga Y, Yamada K, Ogata T, Oka N, Wada T.	Stereocontrolled solid-phase synthesis of phosphorothioate oligoribonucleo- tides Using 2'-O-(2-cyanoethoxymethyl)-nucleoside 3'-O-oxazaphospholidine monomers.	J Org Chem.	77	7913–7922	2012	無
Iwamoto N, Oka N, Wada T.	Stereocontrolled synthesis of oligodeoxyribo- nucleoside boranophosphates by an oxazaphos-pholidine approach using acid-labile N-protecting groups.	Tetrahedron Lett.	53	4361–4364	2012	無
Oka N, Takayama Y, Ando K, Wada T.	Synthesis of nucleoside 5′-borano-phosphorothioate derivatives using an H-boranophosphonate monoester as a precursor.	Bioorg Med Chem Lett.	22	4571–4574	2012	無
Maeda Y, Iwata R, Wada T.	Synthesis of novel oligocationic peptides which bind to A-type nucleic acid duplexes.	Peptide Science 2011.	–	231–232	2012	無
Hari Y, Osawa T, Obika S.	Synthesis and duplex-forming ability of oligonucleotides containing 4'-carboxythymidine analogs.	Org Biomol Chem.	10	9639–9649	2012	無
Kang JH, Tachibana Y, Obika S, Harada-Shiba M, Yamaoka T.	Efficient reduction of serum cholesterol by combining a liver-targeted gene delivery system with chemically modified apolipoprotein B siRNA.	J Control Release.	163	119–124	2012	無

著　者　名	論　文　題　名	雑　誌　名	巻	頁	出版西暦年	GRANTへの謝辞の有無
Yahara A, Shrestha AR, Yamamoto T, Hari Y, Osawa T, Yamaguchi M, Nishida M, Kodama T, Obika S.	Amido-bridged nucleic acids (AmNAs): synthesis, duplex stability, nuclease resistance, and in vitro antisense potency.	Chem Bio Chem.	13	2513–2516	2012	無
Yamamoto T, Yasuhara H, Wada F, Harada-Shiba M, Imanishi T, Obika S.	Superior silencing by 2',4'-BNANC-based short antisense oligonucleotides compared to 2',4'-BNA/LNA-based apolipoprotein B antisense inhibitors.	J Nucleic Acids Res.	–	707323	2012	無
Wada S, Obika S, Shibata M, Yamamoto T, Nakatani M, Yamaoka T, Torigoe H, Shiba M.	Development of a 2',4'-BNA/LNA based siRNA for dyslipidemia and assessment of the effects of its chemical modifications in vivo.	Mol Ther Nucleic Acids.	1	e45	2012	無
Rahman SMA, Baba T, Kodama T, Islam MA, Obika S.	Hybridizing ability and nuclease resistance profile of backbone modified cationic phosphorothioate oligonucleotides.	Bioorg Med Chem.	20	4098–4102	2012	無
Yamamoto T, Harada-Shiba M, Nakatani M, Wada S, Yasuhara H, Narukawa K, Sasaki K, Shibata M, Torigoe H, Yamaoka T, Imanishi T, Obika S.	Cholesterol-lowering action of BNA-based antisense oligonucleotides targeting PCSK9 in atherogenic diet-induced hypercholesterolemic mice.	Mol Ther Nucleic Acids.	1	e22	2012	無

英文総説

著　者　名	論　文　題　名	雑　誌　名	巻	頁	出版西暦年
Oka N, Sato K, Wada T.	Recent progress in the synthesis of glycosyl phosphate derivatives.	Trends in Glycosci. Glycotechnol	24	152–168	2012

邦文単行本

著　者　名	論　文　題　名	書籍全体の編集者名	書籍名	出版社名	(出版地)	頁	出版西暦年
村上正裕，横田隆徳	ビタミンE結合型siRNAの経腸デリバリーによる肝遺伝子発現の抑制	永井恒司、岡田弘晃	ドラッグデリバリーシステムの新展開 II	シーエムシー出版	東京	78–85	2012

Ⅳ.　研究成果の刊行物、別刷

HUMAN GENE THERAPY METHODS 23:119–127 (April 2012)

DOI: 10.1089/hgtb.2012.035

Intrathecal shRNA-AAV9 Inhibits Target Protein Expression in the Spinal Cord and Dorsal Root Ganglia of Adult Mice

Takashi Hirai,[1] Mitsuhiro Enomoto,[1] Akira Machida,[2] Mariko Yamamoto,[2] Hiroya Kuwahara,[2] Mio Tajiri,[2] Yukihiko Hirai,[3] Shinichi Sotome,[1] Hidehiro Mizusawa,[2] Kenichi Shinomiya,[1] Atsushi Okawa,[1] and Takanori Yokota[2]

Abstract

Gene therapy for neurological diseases requires efficient gene delivery to target tissues in the central and peripheral nervous systems. Although adeno-associated virus is one of the most promising vectors for clinical use against neurological diseases, it is difficult to get it across the blood–brain barrier. A clinically practical approach to using a vector based on adeno-associated virus to decrease the expression of a specific gene in both the central and the peripheral nervous system has yet to be established. Here, we analyzed whether upper lumbar intrathecal administration of a therapeutic vector incorporating adeno-associated virus and short-hairpin RNA against superoxide dismutase-1 bypassed the blood–brain barrier to target the spinal cord and dorsal root ganglia. The therapeutic vector effectively suppressed mRNA and protein expression of endogenous superoxide dismutase-1 in the lumbar spinal cord and dorsal root ganglia. Moreover, neither neurological side effects nor toxicity due to the incorporated short-hairpin RNA occurred after the injection. We propose that this approach could be developed into novel therapies for motor neuron diseases and chronic pain conditions, such as complex regional pain syndrome, through silencing of the genes responsible for pathologies in the spinal cord and dorsal root ganglia.

Introduction

THE SPINAL CORD is an important organ for sensory and motor signal processing and is an important anatomical target for neurological disorders, including inflammatory and demyelinating diseases, neurodegenerative diseases, traumatic injury, and neuropathic pain. The delivery of drugs to the spinal cord via systemic administration, such as oral ingestion, intravenous injection, and dermal application, encounters several challenges. Various types of gene therapy vectors have been developed for targeting the central nervous system (CNS). Intravenous injection of a vector based on adeno-associated virus (AAV) can deliver target genes to multiple organs, including the liver and skeletal and cardiac muscle (Mitchell *et al.*, 2000; Gregorevic *et al.*, 2004; Bish *et al.*, 2008). However, delivery of systemically administered AAV to the CNS via the blood–brain barrier has not yet been established, and to avoid systemic side effects, selective administration to the brain or spinal cord is required. Gene therapy trials for Parkinson's disease (Marks *et al.*, 2008), Canavan (Janson *et al.*, 2002), and Batten disease (Worgall *et al.*, 2008) have successfully involved direct brain injection of AAV vectors, but such an invasive method is limited in its application in common clinical practice.

RNA interference (RNAi) has emerged as a powerful tool to induce loss-of-function phenotypes through the posttranscriptional silencing of gene expression (Fire *et al.*, 1998; Dorn *et al.*, 2004). The RNAi pathway is initiated by the enzyme Dicer, which cleaves long, double-stranded RNAs into short (21- to 23-nucleotide) interfering RNA molecules (siRNAs) that mediate sequence-specific gene silencing (Mikami and Yang, 2005; Li *et al.*, 2008). Intraventricular (Senn *et al.*, 2005; Senechal *et al.*, 2007) and intrathecal administration (Luo *et al.*, 2005) of naked or lipid-encapsulated siRNA (Uno *et al.*, 2011) has been used to target the CNS. However, because they still show low transduction efficiencies, insufficient inhibition of gene expression, and short duration of therapeutic effects, these methods are unsuitable for treating chronic neurological disorders (Hassani *et al.*, 2005). To address these

[1]Department of Orthopedic Surgery, Graduate School, Tokyo Medical and Dental University, Tokyo 113–8519, Japan.
[2]Department of Neurology and Neurological Science, Graduate School, Tokyo Medical and Dental University, Tokyo 113–8519, Japan.
[3]Department of Biochemistry and Molecular Biology, Nippon Medical School, Bunkyo-ku, Tokyo 113–0022, Japan.

problems, therefore, viral delivery of short-hairpin RNA (shRNA) expression cassettes that support more efficient and long-lasting transduction into the target CNS is expected to be a promising delivery tool. Local administration methods, such as intramuscular, intrastriatal, and subcutaneous injections, for delivering the viral vector encoding the shRNA have been reported to inhibit target gene expression in mice (Rodriguez-Lebron *et al.*, 2005; Towne *et al.*, 2008; Fu *et al.*, 2009). However, intrathecal injection of shRNA-encoding viral vectors has not yet been documented to reduce the levels of mRNA and protein in the spinal cord and dorsal root ganglia (DRG). To this end, here we show that intrathecal delivery of the AAV-based vector shRNA-AAV9 to mice efficiently inhibited endogenous superoxide dismutase-1 (SOD1), which is ubiquitously expressed in neural tissues.

Materials and Methods

*Construction, production, and titration of anti-*SOD1 *shRNA AAV9 vector*

We prepared the anti-*SOD1* shRNA cassette as previously reported (Yokota *et al.*, 2004; Mayra *et al.*, 2011). The anti-*SOD1* shRNA cassette was cloned downstream of the human polymerase III (Pol III) U6 promoter in the AAV9 vector plasmid (Stratagene, La Jolla, CA). The silencing efficiency of the anti-*SOD1* shRNA sequence was verified using several cultured cell lines and transgenic mice expressing the anti-*SOD1* shRNA, as previously described (Federici *et al.*, 2011). A human growth hormone polyadenylation [hGH poly(A)] cassette (Stratagene) was inserted downstream of the shRNA sequence in the vector for vector titration by quantitative real-time PCR (Fig. 1). The recombinant viral vector was produced according to the three-plasmid transfection protocol and the calcium phosphate method, as previously reported (Hermens *et al.*, 1999).

Animals

All of the animal procedures were performed in accordance with protocols approved by the Animal Experiment Committee of Tokyo Medical and Dental University (Tokyo, Japan) (#81213). Eight-week-old female ICR mice weighing 25–35 g were given intrathecal injections. The animals were divided into two groups: the AAV-treated group (AAV; $n=9$) and the phosphate-buffered saline (PBS)-treated group (PBS; $n=9$). After having been given intraperitoneal injections of chloral hydrate (0.5 mg/g body weight) and ketamine hydrochloride (0.05 mg/g body weight), mice from both the AAV- and PBS-treated groups were placed in the prone position, and a partial laminectomy of the caudal portion of the second lumbar vertebra and the rostral portion of the third lumbar vertebra was performed. The dural matter was exposed and punctured with a 27-gauge needle. Subsequently a PE-10 tube was connected to a 10-μl Hamilton syringe and caudally inserted into the subarachnoid space between these two vertebrae. A volume of 10 μl (6×10^{12} vector genome per microliter) of either the shRNA-AAV9 vector targeting SOD1 or PBS was injected slowly over a 2-min period. After removal of the catheter, the incision was sutured, and the mice were maintained in the head-up position and allowed to recover on a heating pad. The body weights of the mice were measured every week. At 2 and 4 weeks after the injection, all of the mice were killed, and the lumbar spinal cord, lumbar DRG, cardiac muscle, liver, and quadriceps muscle were harvested for analysis. All animal experiments were performed in accordance with the ethical and safety guidelines for animal experiments of the Tokyo Medical and Dental University.

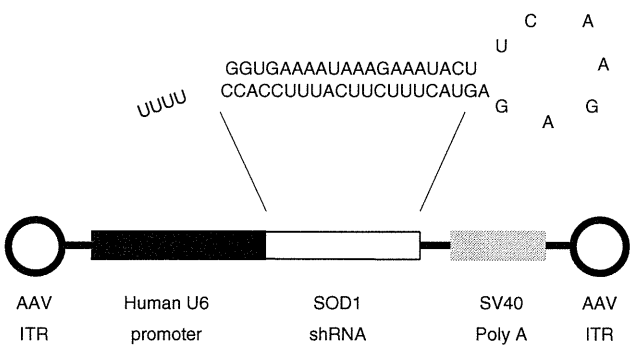

FIG. 1. Construction of the anti-*SOD1* shRNA AAV9 vector. The anti-*SOD1* shRNA expression AAV9 vector, including the anti-*SOD1* shRNA sequence located between the human polymerase III human U6 promoter and the hGH poly(A) cassette, is shown. AAV, adeno-associated virus; hGH, human growth hormone; ITR, inverted terminal repeat; shRNA, short-hairpin RNA; SOD1, superoxide dismutase-1; SV40, simian virus 40.

Measurement of mRNA reduction by quantitative RT-PCR

Total RNA was extracted from the harvested tissues, including the lumbar segment of the spinal cord, the lumbar DRG, cardiac muscle, liver, and the quadriceps muscle, using Isogen (Nippon Gene, Tokyo, Japan). The RNA samples obtained from the lumbar spinal cord were collected from the lumbar region located at the first to second vertebral level. The RNA samples obtained from the DRG consisted of three ganglia, including the fourth, fifth, and sixth lumbar DRG. The DNase I-treated total RNA (0.5 μg) was reverse transcribed, using SuperScript III reverse transcriptase (Invitrogen, Carlsbad, CA). The cDNA was amplified by the quantitative TaqMan system with a LightCycler 480 real-time PCR instrument (Roche, Basel, Switzerland), according to the manufacturer's protocol. The *SOD1* mRNA expression level in each tissue was measured with the following primers and probe: forward primer, 5′-GGTGCAGGGAACCATC-CA-3′; reverse primer, 5′-CCCATGCTGGCCTTCAGT-3′; and probe, 5′-AGGCAAGCGGTGAACCAGTTGTGTTG-3′. Primers for mouse transthyretin (TTR) were designed by Applied Biosystems (Foster City, CA). To normalize the RT-PCR values, the cDNA was also quantitatively amplified with the TaqMan primer and probe sets for glyceraldehyde-3-phosphate dehydrogenase (GAPDH; Applied Biosystems, Warrington, UK). The ratio of *SOD1* mRNA expression to that of GAPDH was calculated to estimate the shRNA silencing efficiency.

Northern blotting analysis of shRNA

RNA was obtained from the lumbar segment of the spinal cord and the lumbar DRG, which were harvested from the bilateral third to sixth lumbar DRG using mirVana (Ambion,

Austin, TX). Five micrograms of RNA derived from the spinal cord and 1 μg of RNA from the DRG were separated on 18% polyacrylamide–urea gels and transferred to Hybond-N+ membranes (GE Healthcare, Piscataway, UK). The blots were hybridized with a probe against the antisense sequence of the shRNA, and the probe sequence was 5′-GGTGGAAATGAAGAAAGTAC-3′. The probe was labeled with a DIG oligonucleotide 3′-end labeling 2nd generation kit (Roche, Penzberg, Germany), and the signal was visualized with a Gene Images CDP-Star detection kit (GE Healthcare).

microRNA expression by quantitative RT-PCR

The expression levels of ubiquitous microRNAs (miRNAs) were measured with miRNA sequence-specific primers (Applied Biosystems, Foster City, CA) and RT-PCR-based detection methodology. Briefly, 100 ng of miRNA collected from the lumbar DRG and spinal cord was reverse transcribed, using PrimeScript RT master mix (Takara Bio, Shiga, Japan) and subsequently amplified with a LightCycler 480 real-time PCR instrument (Roche, Basel, Switzerland). Small nucleolar RNA U6 was used as an endogenous control. The ratio of let-7 or miR-124 expression to that of U6 was calculated to estimate the shRNA silencing efficiency.

Western blotting

A sample from the lumbar spinal cord was collected between the first and second vertebrae, and the DRG sample was extracted from the third, fourth, and fifth lumbar DRG. These tissues were homogenized in cold homogenization buffer containing 0.1% sodium dodecyl sulfate (SDS), 1% sodium deoxycholate, 1% Triton X-100, and 1 m*M* phenylmethylsulfonyl fluoride together with a protein inhibitor cocktail (Roche, Penzberg, Germany). Five micrograms of extracted protein from each sample was mixed with Laemmli sample buffer (Bio-Rad, Hercules, CA), denatured at 37°C for 60 min, and separated on an SDS–15% polyacrylamide gel. The separated proteins were transferred to a polyvinylidene difluoride membrane (Bio-Rad) and were then incubated with specific primary antibodies, including a rabbit anti-SOD1 antibody (Stressgen Biotechnologies, Victoria, BC, Canada) and a mouse anti-GAPDH monoclonal antibody (Biodesign, Saco, ME). After incubation, the membranes were rinsed and incubated with a 0.1% solution of the horseradish peroxidase (HRP)-conjugated secondary antibodies, including goat anti-rabbit HRP IgG and goat anti-mouse HRP IgG (Thermo Science, Rockford, IL). The protein–antibody interactions were visualized with SuperSignal West Femto maximum sensitivity substrate (Thermo Science). The quantification of the band intensity was measured by Scion imaging (National Institutes of Health, Bethesda, MD). We calculated the relative protein expression levels in the lumbar spinal cord and DRG in the AAV-treated group as compared with those in the PBS-treated group.

Histological examinations

Mice were killed by transcardiac perfusion of PBS for 5 min at room temperature, followed by 4% paraformaldehyde (PFA) in PBS for 15 min at 4°C. After perfusion, the lumbar spinal cord and DRG were immediately removed and postfixed in 4% PFA in PBS at 4°C overnight. After fixation, the samples were transferred to PBS containing 30% sucrose and dehydrated for 3 days. The tissues were then embedded in paraffin or low melting temperature agarose (BM Equipment, Tokyo, Japan) in PBS. Ten-micron paraffin sections of the lumbar spinal cord were processed for hematoxylin and eosin and Nissl staining. Frozen sections approximately 20 μm thick from the fifth lumbar (L5) DRG and the spinal cord at the first lumbar vertebral level from mice in each group were incubated for 30 min at room temperature in a blocking solution (5% normal goat serum). The sections were then incubated with a rabbit polyclonal anti-SOD1 antibody (diluted 1:1000; Stressgen Biotechnologies) for 24 hr at 4°C. After incubation, the sections were washed and incubated for 30 min at room temperature with the biotinylated secondary antibody (diluted 1:200; Vector Laboratories, Burlington, ON, Canada) in 0.5% horse serum. The sections were then incubated with ABC reagent (Vector Laboratories) for 30 min, followed by incubation with peroxidase substrate solution for 2 min. After washing, the tissue sections were counterstained with hematoxylin for 1 min.

Rotarod test

The locomotive test was performed with an accelerating Rotarod (Ugo Basile Biological Research Apparatus, Varese, Italy). Mice from both groups were placed on 3-cm rods and were subjected to four trials each day for 4 days. Each trial lasted up to 10 min, and the length of time that the animals could balance on the rod without falling was recorded.

Sensory behavioral tests

The animals were placed in Plexiglas boxes, which were 9.5×21×25 cm in size, to become acclimated to the testing environment. These boxes were then placed on an elevated perforated plastic surface for a minimum of 30 min before all behavioral tests (Hargreaves *et al.*, 1988). A blind observer conducted the behavioral testing.

Tactile threshold. Mechanical sensitivity was measured by applying a series of calibrated von Frey filaments (0.02–8 g) to the plantar aspect of the hind paw. Each filament was applied once to each mouse. Beginning with the 1-g filament, each filament was applied perpendicular to the hind paw for 4–6 sec. A brisk withdrawal of the hind paw indicated a positive response, and the lack of withdrawal indicated a negative response. This filament testing was repeated a maximum of two additional times, and at least two positive responses in three to the filament indicated an overall positive response. If the mouse demonstrated an overall positive response, the next lower force filament was applied as described previously. If no overall positive response was observed (zero or one response in three), the next greater force filament was applied as described previously. Once the crossover threshold could be determined (i.e., from response to no response, or vice versa) the responses to the next five filaments were recorded to determine the median withdrawal threshold.

Response to acetone. Using a plastic tube connected to a 1-ml syringe, and without touching the skin, 100 μl of acetone was applied to the plantar surface of the foot. Acetone

was applied five times to each paw at an interval of at least 30 sec, and the number of brisk foot withdrawals in response to the acetone application was recorded.

Response to noxious heat stimulus. Responses to noxious radiant heat were determined by the Hargreaves method and the Ugo Basile plantar test apparatus. Mice were placed in a transparent plastic chamber on a glass floor and were allowed to acclimate for 30 min. The radiant heat source was placed under the glass floor directly beneath the hind paw. The intensity of the heat stimulus was set to 60 J. Withdrawal latencies were defined as the time between the activation of the heat source and hind paw withdrawal. Withdrawal resulted in the termination of the heat source. A time limit of 15 sec was used to prevent tissue damage. A 5-min interval between consecutive stimulations of the same hind paw was employed. Testing was performed five times on each side, and the latencies for each side were averaged.

Statistical analyses

All data are presented as means ± standard deviation (SD; $n=3$–5). We performed the statistical analysis by Student t test for comparisons between the two groups for all experiments, with the exception of the Rotarod test. For the Rotarod test, the average time of each group was calculated, and statistical significance was assessed by one-way analysis of variance. Significance was defined as p values less than 0.05.

Results

SOD1 mRNA and protein expression in the spinal cord and DRG after lumbar intrathecal administration of shRNA-AAV9

An shRNA-AAV9 vector targeting SOD1 was injected into the subarachnoid space at the second lumbar vertebra of mice to determine the ability of the vector to suppress the expression of SOD1 in the spinal cord and DRG. We first analyzed the efficiency with which *SOD1* mRNA was silenced in various tissues from mice in the AAV-treated group. Quantitative RT-PCR analysis showed that the expression of *SOD1* mRNA in the quadriceps, cardiac muscles, and liver of animals in the AAV-treated group was similar to that of mice that received PBS only (Fig. 2A). However, the level of *SOD1* mRNA in the lumbar spinal cord and DRG of mice in the AAV-treated group was about 60% lower than that in PBS-treated animals (Fig. 2B). These silencing effects in the lumbar spinal cord and lumbar DRG persisted for at least 4 weeks and tended to increase in a time-dependent manner (Fig. 2A). The knockdown effect was specific for the target gene (*SOD1*), given that the levels of other endogenous mRNAs, of GAPDH and TTR, did not change (Fig. 2B), suggesting that shRNA-AAV9 did not affect unrelated endogenous gene expression. Western blot analysis confirmed decreased SOD1 protein levels in the lumbar spinal cord and DRG of shRNA-AAV9–treated mice (Fig. 2C). Four weeks after injection of shRNA-AAV9, the mean level of SOD1 protein expression was 72% lower in the lumbar spinal cord and 68% lower in the lumbar DRG compared with the amounts in PBS-treated mice (Fig. 2D). Immunohistochemical analysis with anti-SOD1 antibody confirmed silencing of SOD1 within the lumbar spinal cord and DRG. The SOD1 immunoreactivity of the lumbar spinal cord and DRG was much lower in the AAV-treated group than in the PBS-treated group (Fig. 2E).

Robust delivery of shRNA-AAV9 to the lumbar spinal cord and DRG, and detection of siRNA derived from shRNA encoded by AAV9 in these tissues

To investigate whether shRNA-AAV9 was delivered to the lumbar spinal cord and DRG, we used Northern blotting to examine the expression of anti-*SOD1* shRNA in these tissues. The 54-nucleotide intact shRNA was not present, but a 21-nucleotide antisense strand of siRNA was detected in both tissues (Fig. 2F). This finding clearly indicated that the shRNA encoded by AAV9 was in fact delivered to the cytosol of target cells and that the expressed anti-*SOD1* shRNA was almost completely processed by Dicer.

Endogenous miRNA expression in the lumbar spinal cord and DRG after intrathecal injection of shRNA-AAV9

Because both RNA forms share intracellular machinery for their expression in mammalian cells, we sought to clarify whether overexpression of shRNA decreased the processing of endogenous miRNA (Grimm *et al.*, 2006; Rossi, 2008). To this end, we used quantitative RT-PCR to evaluate the expression levels of representative miRNAs (let-7 and miR-124) in the lumbar spinal cord and DRG. Expression levels of let-7 and miR-124 (Fig. 3A) were similar in PBS- and AAV-treated mice. These results indicate that the endogenous miRNA pathway was preserved in the lumbar spinal cord and DRG after injection of shRNA-AAV9.

Histological evaluations of the lumbar spinal cord and DRG

We histologically evaluated whether any anatomical abnormalities occurred in the lumbar spinal cord and DRG after shRNA-AAV9 injection. Hematoxylin and eosin staining of these tissues showed no inflammation, necrosis, or degenerative lesion formation (Fig. 3B). In addition, Nissl staining revealed no structural neuronal deterioration after injection of shRNA-AAV9 (Fig. 3B).

Body weight and locomotive and sensory functions

To assess the general health and motor and sensory functions of the hind limbs of mice after injection of PBS or shRNA-AAV9, we observed these animals for 2 to 4 weeks after treatment. Body weights of the mice in the AAV-treated group were similar to those in the PBS-treated group (Fig. 4A). In addition, accelerating Rotarod tests revealed no significant differences in motor function between the PBS- and AAV-treated mice (Fig. 4B). Furthermore, there were no significant differences between groups, either before or after treatment, according to the thermal (Fig. 4C), tactile (Fig. 4D), and acetone (Fig. 4E) tests.

Discussion

Successful neuronal transduction vectors targeting the CNS have been developed (Fu *et al.*, 2003, 2011; Puskovic *et al.*, 2004). Among the viral vectors used for gene transfer,

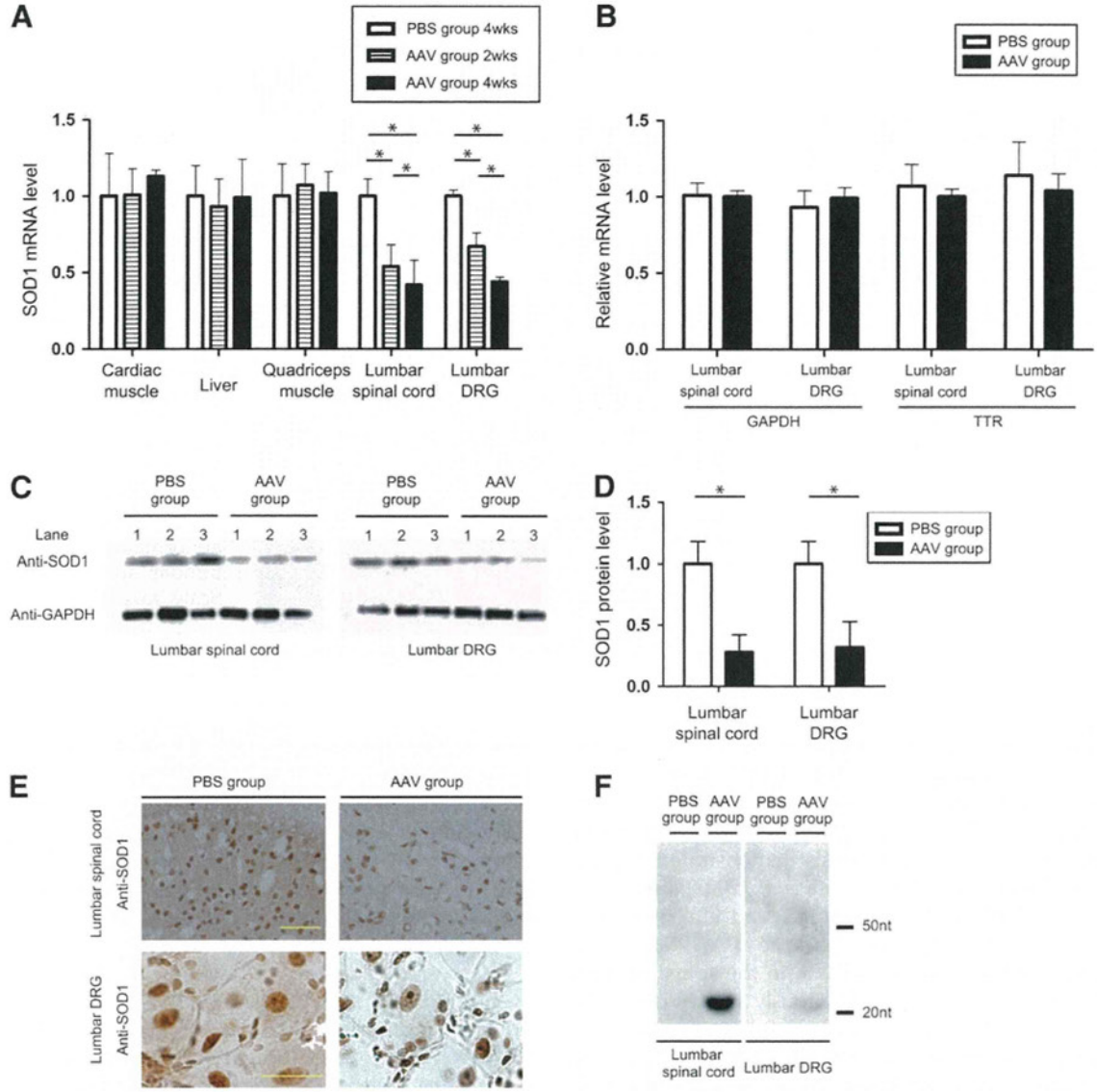

FIG. 2. Expression of *SOD1* mRNA in various tissues, reduction of SOD1 protein expression, and expression of *SOD1* shRNA in the lumbar spinal cord and DRG of mice. **(A)** Quantitative RT-PCR analysis of *SOD1* mRNA expression in cardiac muscle, liver, quadriceps muscle, lumbar spinal cord, and lumbar DRG in mice 2 and 4 weeks after injection of PBS (control) or the shRNA-AAV9 vector. *SOD1* mRNA expression was significantly ($*p < 0.05$) inhibited in the lumbar spinal cord and DRG of the AAV-treated group 2 weeks after injection. In addition, expression was reduced in a time-dependent manner. Data are presented as means ± 1 SD ($n = 4$ or 5 mice per group). **(B)** Quantitative RT-PCR analysis of endogenous mRNAs (of *TTR* and *GAPDH*) in the lumbar spinal cord and DRG (removed 4 weeks after injection) relative to total input RNA. Data are presented as means ± 1 SD ($n = 4$ or 5 mice per group; $*p < 0.05$). **(C** and **D)** SOD1 protein levels of three mice, as assessed by Western blot analysis 4 weeks after injection of PBS or shRNA-AAV9. Data are presented as means ± 1 SD ($n = 3$ mice per group; $*p < 0.05$). **(E)** Expression of SOD1 based on immunohistochemical analysis in the lumbar spinal cord and lumbar DRG. **(F)** Northern blotting analysis of total RNA derived from the lumbar spinal cord and DRG, 4 weeks after injection of PBS or shRNA AAV9. The 21-nucleotide antisense bands indicative of functional siRNA were detected. DRG, dorsal root ganglia; GAPDH, glyceraldehyde-3-phosphate dehydrogenase; SOD1, superoxide dismutase-1; TTR, transthyretin. Color images available online at www.liebertpub.com/hgtb

AAV vectors have the advantage of conferring stable, long-term gene expression in the absence of an inflammatory response (Kaemmerer *et al.*, 2000). Therefore, AAV vectors have been used for gene therapy targeting neurological disorders, and the different transduction abilities of various AAV vector serotypes have been investigated. The AAV9 vector has the highest infectivity for neural tissue in a rodent model (Storek *et al.*, 2008; Bevan *et al.*, 2011; Federici *et al.*, 2011). Among AAV serotypes, including AAV1, AAV6, and AAV8, intrathecal injection of an AAV9 vector encoding green fluorescent protein is the most effective for biodistribution and transduction in the spinal cord and DRG of mice (Storek *et al.*, 2008; Snyder *et al.*, 2011). We therefore chose AAV9 as the vector for gene delivery to the spinal cord and DRG and found that it stably expressed the transgene in both tissues.

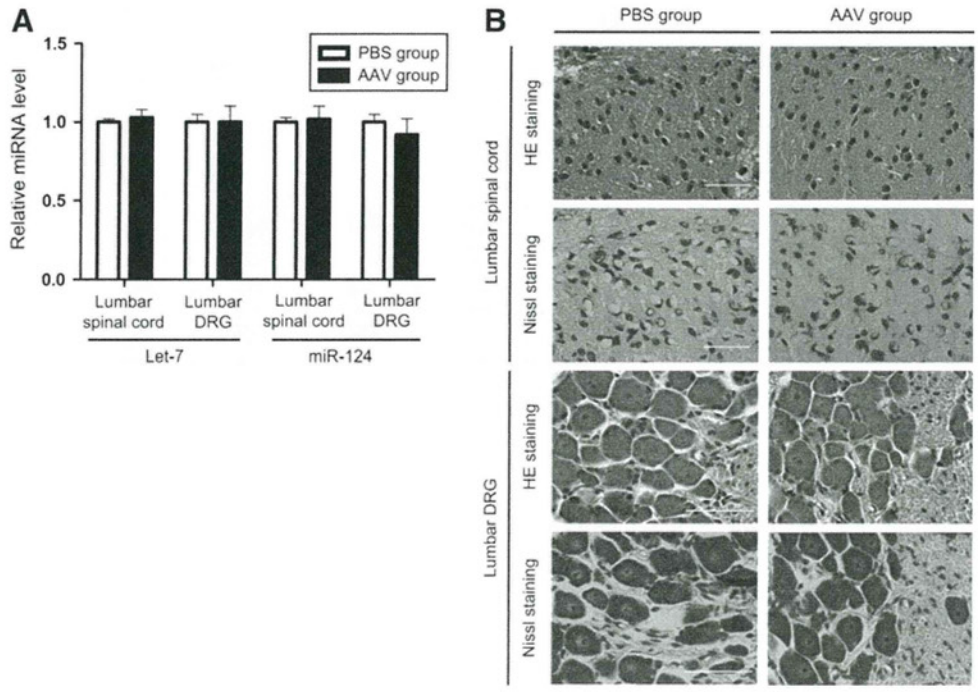

FIG. 3. Lack of change in the expression of endogenous miRNAs in the lumbar spinal cord and dorsal root ganglia (DRG), and absence of histological abnormalities in these structures, after shRNA-AAV9 injection. **(A)** Quantification of endogenous levels of the miRNAs let-7 and miR-124 in the lumbar spinal cord and DRG, determined by quantitative RT-PCR. Data are presented as means ± 1 SD ($n = 3$ mice per group; $^*p < 0.05$). **(B)** Hematoxylin–eosin (HE) and Nissl staining were done to demonstrate the absence of abnormalities in either the lumbar spinal cord or DRG. Scale bars: 50 μm.

We chose *SOD1* as the target gene in the spinal cord, because siRNA targeting wild-type *SOD1* halts familial amyotrophic lateral sclerosis (ALS) caused by *SOD1* mutation by silencing the mutant gene in siRNA-expressing transgenic mice, as we had previously demonstrated as proof of principle (Saito *et al.*, 2005; Yokota *et al.*, 2007). Moreover, we think that *SOD1* is an appropriate and effective endogenous gene for evaluating side effects due to AAV-associated toxicity and overexpression of shRNA in the spinal neurons and DRG, because *SOD1* is ubiquitously expressed in the CNS and because *SOD1* knockout mice exhibit no neurological phenotypes except for enhanced susceptibility to axonal injury and cerebral ischemia (Reaume *et al.*, 1996; Kawase *et al.*, 1999).

Our results demonstrated that intrathecal administration of shRNA-AAV9 reduced the mRNA expression levels of the targeted molecule by approximately 60% in both the spinal cord and the DRG, and that this reduction persisted for at least 4 weeks.

Although this reduction might not be considered robust, it may be sufficient to alter an associated phenotype in mice. Even partial reduction of SOD1 production in the spinal cord is suggested to have a substantial therapeutic effect on the ALS phenotype, because the copy number of the mutant transcript (G93A SOD1) and the severity of the ALS phenotype are closely associated in SOD1G93A transgenic mice. (Alexander *et al.*, 2004) Similarly, in the DRG, partial knockdown of transient receptor potential vanilloid-1 (TRPV1) by about 75% in shRNA-transgenic mice decreases the development of inflammatory thermal hyperalgesia after spinal nerve ligation (Christoph *et al.*, 2008). These results indicate that even modest reduction of target gene expression may be sufficient for effective gene therapy. Moreover, excess expression of shRNA, to the extent that target gene expression is nearly completely suppressed, may outcompete miRNA or pre-miRNAs and oversaturate components of the endogenous miRNA processing machinery, such as exportin-5 and Ago2, resulting in cellular damage due to miRNA deficiency (Grimm *et al.*, 2006; Rossi, 2008). In the current study, the expression of endogenous miRNAs was unchanged after administration of shRNA-AAV9, suggesting that the viral dose we used might have been sufficient for a silencing effect and might have fallen within the therapeutic window, where toxicity does not occur.

One possible strategy for "tuning" the shRNA expression level is the use of inducible promoters such as the tetracycline-inducible promoter (Kappel *et al.*, 2007). In this situation, expression of the shRNA might be "switched on" temporarily through the systemic addition of doxycycline but "switched off" (e.g., when the silencing effect is excessive or shRNA toxicity is observed) by withdrawal of doxycycline. Thus, the silencing effect on the target gene after intrathecal injection of shRNA-AAV9 might be adjusted on demand through the use of an inducible promoter for shRNA expression.

Although we confirmed that the gene-silencing effect in the spinal cord and DRG persisted for as long as 4 weeks in our mice, we did not examine persistence beyond this time point. The protein expression that is induced systemically after AAV injection has been reported to reduce target gene expression in humans for months, and this result likely reflects immunological elimination of shRNA-AAV complexes by $CD8^+$ memory T cells (Peden *et al.*, 2004; Yokota *et al.*, 2004; Manno *et al.*, 2006). However, AAV vector constructs that are injected directly into the CNS are well known to show prolonged expression of their transgenes without the induction of an immune response (Janson *et al.*, 2002; Marks *et al.*, 2008; Worgall *et al.*, 2008). In addition, we previously demonstrated that shRNA-transgenic mice that expressed the same shRNA as used in the present study showed significant suppression of *SOD1* for longer than 1 year (Saito *et al.*, 2005). Accordingly, we believe that the AAV vector we used here can stably express the transgene